

Solving 2D Coupled Water Entry Problem by an Improved MPS Method

Ruosi Zha, Heather Peng and Wei Qiu*

Department of Ocean and Naval Architectural Engineering, Memorial University of Newfoundland, St. John's, Canada

* E-mail: qiuw@mun.ca

1 INTRODUCTION

It is important to understand fluid-structure interactions (FSI) for a ship or offshore structure under slamming loads, wave impact and/or green water. Hydrodynamic aspects of these types of nonlinear loads on ships and offshore-structures have been widely studied. Studies on the interactions between structural responses and these highly nonlinear loads are relatively rare. For water-entry problems, Panciroli et al. (2012) studied the hydroelastic effect by conducting a series of the experimental tests on an elastic wedge entering the calm water. In their work, effects of entry velocity, structural material, and plate thickness on the strain of the wedge plate were examined. Iafrati (2016) carried out experiments to investigate the water impact loads on deformable plates with different stiffness.

Despite the success in numerical solutions, difficulties still exist in addressing high nonlinearities, breaking surfaces and irregular fluid-structure interfaces. The Lagrangian particle-based methods are promising to simulate hydroelastic responses of structures under slamming loads, involving breaking free surfaces and variable fluid-structure interfaces. For example, Panciroli et al. (2012) applied the smoothed particle hydrodynamics (SPH) method to study the water entry problems of deformable wedges. The moving particle semi-implicit (MPS) method solves the Poisson equations for pressure and allows for better pressure prediction using a larger time step size. Hashimoto and Le Touzé (2014) developed a coupled MPS-FEM model to solve a violent flow-structure interaction problem. Kondo et al. (2007) and Hwang et al. (2014) used the MPS method to solve elastic structural responses. Sun et al. (2015) developed a modified version of MPS and applied it to simulate 2D dam breaking and the flow interaction with rigid and flexible structures.

In the present work, an improved MPS method was developed to solve the hydroelastic response of a wedge entering calm water. The improved method addressed issues associated with the pressure calculation and the numerical stability. A more accurate scheme was developed to identify the free surface particles near wall boundary and the fluid-structure interface. Instead of determining the interface by interpolation, the wall particles and the structural particles on the interface layer were considered as the interface particles to avoid additional computational burden. This simplified interface treatment also allows for the utilization of different particle spacing/size for the fluid and the structure. Preliminary convergence studies were carried out using various numbers of particles. Numerical solutions were compared with experimental data (Panciroli et al., 2012) in the initial validation studies.

2 NUMERICAL FORMULATION

The governing equations for incompressible viscous flow are given in Eq. 1 and Eq. 2. For isotropic elastic structures, the governing equations, based on the conservation of momentum and angular momentum, are presented in Eq. 3 and Eq. 4.

$$\frac{1}{\rho_f} \frac{D\rho_f}{Dt} + \nabla \cdot V_f = 0 \quad (1)$$

$$\frac{DV_f}{Dt} = -\frac{1}{\rho_f} \nabla P + \nu_f \nabla \cdot \nabla V_f + g + \frac{1}{\rho_f} F_{s-f} \quad (2)$$

$$\frac{DV_s}{Dt} = \frac{1}{\rho_s} \nabla \cdot (\mathbf{p} + \boldsymbol{\sigma}) + g + \frac{1}{\rho_s} F_{f-s} \quad (3)$$

$$\frac{D}{Dt} (I_s \omega_s) = \frac{D}{Dt} (r_s \times (m_s V_s)) \quad (4)$$

where ρ_f is the density of fluid; ρ_s denotes the density of the structure; and V_f, P, g and F_{s-f} represent the fluid velocity, the fluid pressure, the gravitational acceleration, and the structural force on fluid, respectively. In Eqs. 3 and 4, $V_s, \mathbf{p}, \boldsymbol{\sigma}, I_s, m_s, \omega_s$ and r_s are the velocity, the isotropic pressure, the stress tensor, the moment of inertia, the mass, the angular velocity, and the position vector of a structural particle, respectively; and F_{f-s} denotes the fluid force on structure. Details on the discretization and the solution of the governing equations by the MPS method can be found in the work of Hwang et al. (2014).

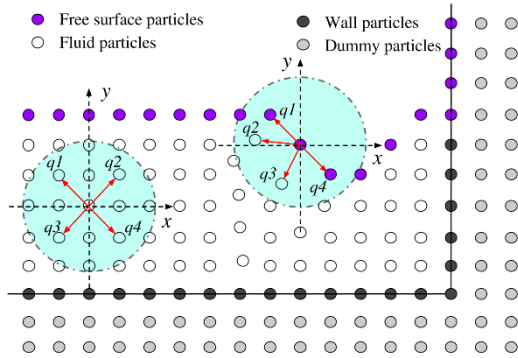


Fig. 1 Modified scheme for free surface identification

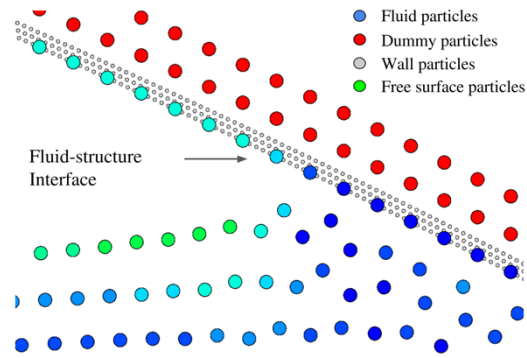


Fig. 2 Treatment of fluid-structure interface

3 IMPROVED MPS METHOD

To overcome the drawbacks of the original MPS method, various improvements have been made by many researchers. Details can be found in the work of Gotoh and Khayyer (2016), in terms of the kernel function, the computation of pressure gradient, the Laplacian operator, the Poisson equations for pressure, the identification of free surface, the collision model, and the treatment of fluid-structure interface. To improve the particle identification, Zhang et al. (2013) proposed an approach using non-symmetric neighboring particles. However, this approach could misidentify the free surface particles for wall particles. An improved scheme was developed in this work to avoid false identification, in which the non-symmetric particle approach was used for the fluid particles and the density criteria was applied to the wall particles as illustrated in Fig. 1. A pairwise collision model by Lee et al (2011) was adopted to keep two particles from being too close each other and therefore the numerical stability was improved.

In the present studies, two types of particles with different sizes were used in discretizing the governing equations for fluid and structures, respectively, to improve computing efficiency and accuracy. In this case, the structural particles cannot be directly considered as the wall and the dummy particles for fluid analysis. The treatment of the fluid-structure interface is shown in Fig. 2, where a small circle represents a structural particle and larger circles denote fluid particles, wall particles and their dummy particles. Consequently, the fluid-structure interface includes two types of particles - the wall particles and the structural particles on the interface layer. The pressures for the wall particles can be directly obtained by solving the Poisson equations, while the pressures for the structural particles on the interface can be interpolated from those for their adjacent wall particles.

In the computation, the fluid and structural particles are treated separately. The governing equations for the fluid are solved first. After the pressures for the interface particles are computed, the fluid forces on the structure are obtained by integrating the pressures. The positions of the interface particles are then updated according to the structural computations. The updated information for the wall particles in the flow analysis is then used to form the new boundary conditions for the computation at the next time step.

4 VALIDATION STUDIES

Validation studies were carried out for the elastic wedge tested by Panciroli et al. (2012). In their work, the structural deformations were measured for various the wedge thicknesses, deadrise angles, and impact velocities. The wedge was made of two aluminum panels (300 mm long, 250 mm wide and 2 mm thick) with rigid connection only at the wedge tip. The test results for the elastic wedge were used in the validation studies. The density of aluminum was $2,700 \text{ kg/m}^3$, its Young's modulus was $E=68 \text{ GPa}$, and the Poisson ratio was $\nu=0.3$. The deadrise angle of the wedge was 30° and two strain gauges were located at 30 mm and 120 mm from the tip on each side of the wedge.

The computational conditions were set as the same as those in the experiments. The computational domain and the initial particle settings are given in Fig. 3. The domain width was set as 1.6 m and the water depth was 0.6 m. To save computational time, the numerical simulation started from the time instant of impact with an initial entry velocity of 4.0 m/s relative to the calm water, corresponding to an equivalent dropping height of 0.8155 m.

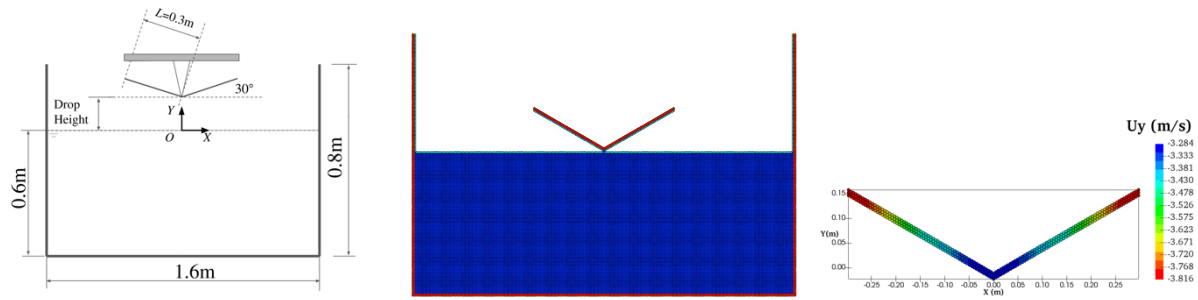


Fig. 3 Computational domain, the initial distribution of particles and the velocity contour at $t=0.006$ s

The convergence of the predicted strain to the number of particles was investigated by using three numbers of particles, as presented in Table 1, varying from 29,517 to 36,093. In Case 1, the ratio between the spacing of the fluid particle and that of the structural particle was 3.0. In other two cases with more particles, the ratios were increased to 5.0, i.e., more structural particles were used for structural analysis. In all the three cases, the time step for the flow analysis was set as 2×10^{-5} s. A smaller time step was employed for the structural solution. Note that the smaller particle spacing for the structure requires smaller time step to meet the CFL condition and a very small time step was required to deal with the large accelerations of structural particles. The time step size for structural analysis was then set as 2×10^{-7} s. The time history of the strain at the location of 30 mm from the wedge tip is presented in Fig. 4. The predicted strain converged as the numbers of fluid and structural particles were increased.

Table 1 Numbers of Particles used in Convergence Studies

Case No.	Number of fluid particles	Number of structure particles	Total number
1	27,270	903	29,517
2	30,388	1593	32,755
3	33,600	1683	36,093

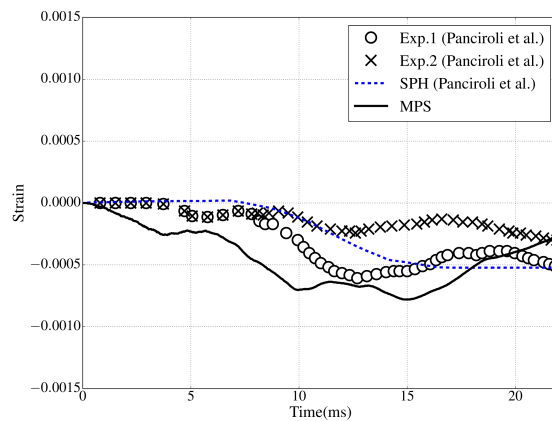
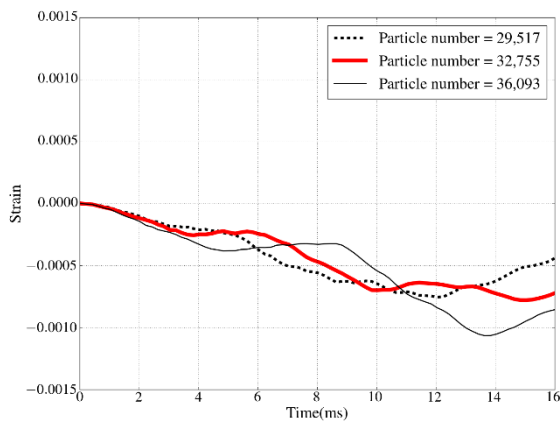


Fig. 4 Computed strains using different numbers of particles Fig. 5 Comparison with experimental and SPH results

Figure 5 presents the computed strain at the same location using 32,755 particles and its comparison of the experimental data and the results by SPH (Panciroli et al., 2012). The computed strain of the deformed wedge panel indicates a good trend in comparison with the experimental data and the numerical results, but with discrepancies at earlier and later stages of the impact. It could be due to insufficient number of structural particles across the thickness direction of the wedge panel. More results will be presented at the Workshop using more particles along the thickness direction.

The strain distributions on the deformable wedge panels and the wedge deformations at four time instants are presented in Fig. 6. At $t=0.00$ s, the strain was zero over the whole wedge panels. At $t=0.01$ s, the wedge tip was subjected to the impact pressure and large strains occurred in the area near the wedge tip. The strains were relatively small in other areas of the panels with slightly decreased deadrise angles. The snapshots at $t=0.02$ s and $t=0.026$ s show that the strain near the wedge tip decreased with the increase of the wetted area. The deadrise angle at each location tended to restore to its initial value. Extended simulation will be performed to examine the strain and deformation of the wedge up to the time instant when it is completely submerged.

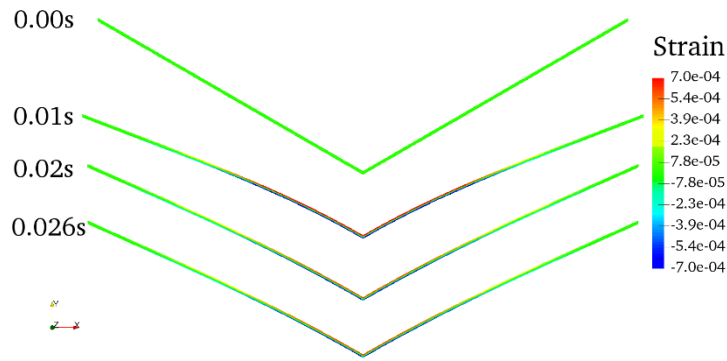


Fig. 6 Strain contour over the wedge panels at various time instants

5 CONCLUSIONS

A modified MPS method with two main improved schemes was developed to solve a 2D fluid-structure interaction problem. In the first scheme, the criteria for free surface identification was revised. The second improved scheme involved the treatment of the fluid-structure interface and the use of two different particle spacing/size values for fluid and structural analysis. Preliminary validation studies were carried out for an elastic wedge entering calm water. The computed strain was compared with experimental data and those by SPH. More numerical results for different initial entry velocities, deadrise angles and at more strain sensor locations will be presented at the Workshop.

ACKNOWLEDGEMENTS

This work was supported by the Natural Science and Engineering Research Council (NSERC) of Canada.

REFERENCES

- Gotoh, H., and Khayyer, A., 2016. Current achievements and future perspectives for projection-based particle methods with applications in ocean engineering. *Journal of Ocean Engineering and Marine Energy*, pp. 1–28.
- Hashimoto, H., and Le Touzé, D., 2014. Coupled MPS-FEM model for violent flows-structures interaction. In *Proceedings of the 29th IWWF*.
- Hwang, S. C., Khayyer, A., Gotoh, H., and Park, J. C., 2014. Development of a fully Lagrangian MPS-based coupled method for simulation of fluid-structure interaction problems. *Journal of Fluids and Structures*, 50, pp. 497–511.
- Iafrafi, A., 2016. Effects of plate stiffness on fluid-structure interaction in high-speed plate ditching. In *Proceedings of the 31th IWWF*.
- Kondo, M., Tanaka, M., Harada, T., and Koshizuka, S., 2007. Elastic objects for computer graphic field using MPS method. In *ACM SIGGRAPH 2007 posters*, ACM, p. 53.
- Lee, B. H., Park, J. C., Kim, M. H., & Hwang, S. C., 2011. Step-by-step improvement of MPS method in simulating violent free-surface motions and impact-loads. *Computer methods in applied mechanics and engineering*, 200(9), pp. 1113-1125.
- Panciroli, R., Abrate, S., Minak, G., and Zucchelli, A., 2012. Hydroelasticity in water-entry problems: Comparison between experimental and SPH results. *Composite Structures*, 94(2), pp. 532–539.
- Sun, Z., Djidjeli, K., Xing, J. T., and Cheng, F., 2015. Modified MPS method for the 2D fluid structure interaction problem with free surface. *Computers & Fluids*, 122(2015), pp. 47–65.
- Zhang, Y., Wang, X., Tang, Z., and Wan, D., 2013. Numerical simulation of green water incidents based on parallel MPS method. In *Proceedings of the Twenty-third International Offshore and Polar Engineering Conference*, ISOPE, pp. 931–938.